

1-1-2022

Mineralogical and geochemical signatures of weathering on carbonate rocks and dynamic young land surfaces in Muğla Polje (SW Turkey)

CEREN KÜÇÜKUYSAL

MURAT GÜL

TURAL AGHAYEV

MERVE GÜLCAN

Follow this and additional works at: <https://journals.tubitak.gov.tr/earth>



Part of the [Earth Sciences Commons](#)

Recommended Citation

KÜÇÜKUYSAL, CEREN; GÜL, MURAT; AGHAYEV, TURAL; and GÜLCAN, MERVE (2022) "Mineralogical and geochemical signatures of weathering on carbonate rocks and dynamic young land surfaces in Muğla Polje (SW Turkey)," *Turkish Journal of Earth Sciences*: Vol. 31: No. 6, Article 4. <https://doi.org/10.55730/1300-0985.1820>

Available at: <https://journals.tubitak.gov.tr/earth/vol31/iss6/4>

This Article is brought to you for free and open access by TÜBİTAK Academic Journals. It has been accepted for inclusion in Turkish Journal of Earth Sciences by an authorized editor of TÜBİTAK Academic Journals. For more information, please contact academic.publications@tubitak.gov.tr.

Mineralogical and geochemical signatures of weathering on carbonate rocks and dynamic young land surfaces in Muğla Polje (SW Turkey)

Ceren KÜÇÜKUYSAL*, Murat GÜL, Tural AGHAYEV, Merve GÜLCAN

Department of Geological Engineering, Faculty of Engineering, Muğla Sıtkı Koçman University, Muğla, Turkey

Received: 02.07.2022

Accepted/Published Online: 16.10.2022

Final Version: 16.11.2022

Abstract: Red soils as the weathering products in Muğla Polje (SW Turkey) show different occurrences either on hard and permeable limestone (terra rossa (TRs)) or within the matrix of transported sediments (alluvium-derived soils (ALs), alluvium-derived soils specifically from clastics (ALsc), paleosol (Pls), and colluvium-derived soils (CLs)). The purpose of this study is to unlock the effect of weathering on hard carbonate rocks and dynamic young land surfaces (alluvium and colluvium) in Muğla Polje for the first time in terms of mineralogical and geochemical compositions. TRs, the soils of more stable environments are clayey while ALs and CLs as being the soils of dynamic environments have variable textures from silty clay loam to sandy loam. All soils share low CEC property (13–16.8 meq/100 g for TRs; 2–11.6 meq/100g for ALs and CLs). Nonclay components of the samples include quartz, feldspars, calcite, dolomite, and mica minerals. Hematite is observed as the main reddening agent for all samples. Illite, kaolinite, chlorite, and vermiculite are the clay minerals of the fine fractions. TRs are characterized by low intensity of salinization (<1) and calcification (<2), high degree of clayeyness (>0.3), and intense hydrolysis due to very high CIA and CIA-K (84%–88% and 89%–93%) under very high MAP (1230–1285 mm year⁻¹). ALs and CLs are the soils with moderate to high calcification (>2), low salinization (<1), high base amounts (70–522; 73–141), low intensity of leaching developed under low CIA and CIA-K (3%–22% and 10%–16%) due to low MAP (<270 and <197 mm year⁻¹). Samples of Pls and ALsc are also qualified with low salinization (<1), low calcification (<2), and intense leaching (>0.2) associated with very high CIA and CIA-K (>80%, >90%) under very high MAP (>1260 mm year⁻¹). Therefore, this study suggests that TRs are the results of intense weathering on carbonate rocks of more stable environments while ALs and CLs are the products of weathering of much lower intensity on alluvium and colluvium. As more mature soils of the polje, TRs also contribute to the matrix of the transported sediments in the lowlands of the polje.

Key words: Terra rossa, red Mediterranean soil, chemical weathering, molecular weathering ratio

1. Introduction

The common name for the red-colored soils developed under the Mediterranean climate has been assigned as “red Mediterranean soils (RMs)” or “terra rossa soils (TRs)” for those that develop either along with the fractures of the limestones and dolomites in the karstic terranes or as a red stratum on and between the transported parent materials (Yassoglou et al., 1997; Durn, 2003; Miko et al., 1999; Torrent, 2005; Merino et al., 2006; Priori et al., 2008; Vingiani et al., 2018). According to the soil nomenclature, these soils are mostly classified as Rhodoxeralfs (USDA, 1994) and Chromic Luvisol (WRB, 2015). Two main pedogenic processes; rubification (Boero and Schwertmann, 1989) and clay illuviation are suggested to be critical for the development of special characteristics of TRs (Yaalon, 1997; Torrent, 2005; Fedoroff and Courty, 2013). Reddening is proposed to be due to the presence of Fe-oxide minerals (hematite/goethite) (Eren and Kadir, 2013; Feng et al., 2018).

* Correspondence: cerenkucukuyisal@mu.edu.tr

Some studies suggest that TRs develop widely from the insoluble residues of carbonate rocks (Moresi and Monghelli, 1988; Atalay, 1997; Wei et al., 2013); some others recommend the contribution of external materials, e.g., aeolian dust, volcanic debris, clastic sedimentary fragments, etc. (Muhs et al., 2012; Sandler et al., 2015). However, the widely accepted theory is the polygenetic nature of TRs which comprises all mentioned pedogenetic formations (Bronger and Bruhn-Lobin, 1997; Durn et al., 1999; 2014; Lucke, 2008).

RMs or TRs across Anatolia through the karstic terranes have also been studied (e.g., Özbek et al., 1976; Kapur et al., 1993; Kubilay et al., 1993; Eren and Kadir, 1999; Aydınlı and Cresser, 2008; Aydınlı and Fitzpatrick, 2009; Bolca et al., 2012). Although the karstic depressions in southwest Turkey have been recognized for the occurrences of TRs, a limited number of studies have been carried out to understand the genesis and the

composition of such soils. Muğla Polje, one of these karstic depressions, includes two different occurrences of red soils: (1) TRs developed on hard and permeable carbonate rocks and (2) the soils formed the matrix of the transported sediments (alluvium-ALs and colluvium-CLs). TRs being the soils of a more mature and stable paleoenvironment, and ALs-CLs representing the young land surfaces (flood plains, landslide debris) have comparable features that can help to reveal the effect of parent rock compositions on the soil formations. Therefore, the main goal of this study is to compare the effect of weathering on hard carbonate rocks (limestone and dolomite) and dynamic young land surfaces (floodplain and landslide debris) in Muğla Polje in terms of mineralogical and geochemical compositions.

2. Materials and methods

2.1. Field descriptions

Muğla Polje with a 40 km² area at an elevation between 618 and 653 m is a very typical karstic depression located in southwest Turkey (Figure 1A). According to the Muğla weather station-17292 of the Turkish State Meteorological Service, the mean annual temperature is 15.1 °C with the warmest month being August (33.5 °C) and the coldest month being January (1.6 °C). Additionally, the annual rainfall is 1208.3 mm with a maximum in November (265.5 mm) and a minimum in July (11.7 mm). Based on the Köppen classification, the climate of the study area is of humid Mediterranean climate (Csa) with long, hot, and dry summers and cool and wet winters.

Muğla Polje is filled with colluviums-slope debris and alluvial fan deposits at the margins, especially on the northern side, and alluvial deposits at the polje interiors. The oldest unit exposed around the polje is the Permo-Carboniferous schist which has an outcrop at the south of the study area (Figure 1B). To the southeast, the Mid-Triassic-Liassic dolomite, red-colored basal conglomerate; metasandstone, metasiltstone, and dolomitic limestone are followed by Jurassic-Lower Cretaceous limestone and Upper Cretaceous-Paleocene cherty limestone and end with sandstone-limestone-shale (Figure 1B) (Göktaş, 1998). The Liassic limestone-dolomite are the most widespread units exposed in the study area (Figure 1B) (Göktaş, 1998; Gül, 2015). Younger units are the Oligocene(?) -Lower Miocene clastics (Göktaş, 1982, 1998; Göktaş et al., 1982) and the Upper Miocene-Pliocene red-colored limestone fragments with conglomerate, sandstone, and mudstone alternations (Figures 1B; Gül et al., 2013). Quaternary deposits are dominantly of colluviums-alluvial fan deposits-alluviums (Figure 1B; Atalay, 1980; Göktaş et al., 1982; Konak et al., 1987; Aktimur et al., 1996; Göktaş, 1998; Gül, 2015; Gül et al., 2021).

The sampling locations were determined based on the significance and accessibility of the sites and the sampling

was mostly undertaken along the wall/floor of the road cuts. The surfaces were cleaned prior to field observations and sampling. The horizon/section depths of the water-laid deposits were recorded from zero datum at the ground surface; while the sampling from the fractures/cracks was reported as the depth of the sample point from the surface (Schoeneberger et al., 2012). The profiles and the sampling points are dominantly covered with maquis and pine trees.

Information about the sampling sites, their environmental settings, and types of parent and bedrocks are provided in Table 1. Soils developed from the parent rocks of alluvium enriched in clastic components are specifically named as ALsc. In addition, one paleosol (buried soil) sample within 1st location of ALs is symbolled as Pls in this study. ALs refer to all alluvium-derived soils including ALsc and Pls unless they are specifically mentioned in the paper. A total of 12 representative sites within the study area were selected to investigate. In particular, TRs samples (2nd, 4th, 10th, and 14th sites) were obtained from the fractures of parent rocks or as a red stratum over the Liassic limestone and the Middle Triassic-Liassic dolomite (Figure 2). ALs samples were taken from the profiles having bedrocks of alluviums; more specifically defined as ALs fed by the Liassic limestone (1st, 7th, 8th, and 13th sites) and ALsc (11th and 12th sites) originated from the Oligocene (?) -Lower Miocene conglomerate – sandstone and to a lesser extent Liassic limestone and Campanian-Maastrichtian cherty limestone. CLs samples (6th and 9th sites) lay down along a colluvial wedge on the Liassic limestone (Aktimur et al., 1996; Göktaş, 1982, 1998; Göktaş et al., 1982; Gül, 2015; Konak et al., 1987) (Figure 2).

2.2. Laboratory analysis

Thin sections of the parent rocks were prepared at Mineralogy-Petrography Laboratory at General Directorate of Mineral Research and Exploration (MTA) to describe mineralogical and petrographical properties under a polarizing microscope.

Soil samples were dried at room temperature and then gently crushed and sieved through a 2-mm sieve. The grain size distribution of the samples was determined using soil hydrometer 152H based on the ASTM D7928 method, and cation exchange capacity (CEC) of <63 µm fraction of each sample was measured by methylene blue test according to the method of Jones (1964) at Clay Mineralogy Laboratory at Muğla Sıtkı Koçman University.

Soil samples were analyzed mineralogically by a Panalytical Expert Pro diffractometer equipped with a Cu tube at 40kV voltage and 30mA current with a scanning rate of 2°/min at Mineralogy-Petrography Laboratory at MTA. The clay fraction of the samples was separated with sedimentation followed by centrifugation. The diffractograms of whole-rock samples were plotted

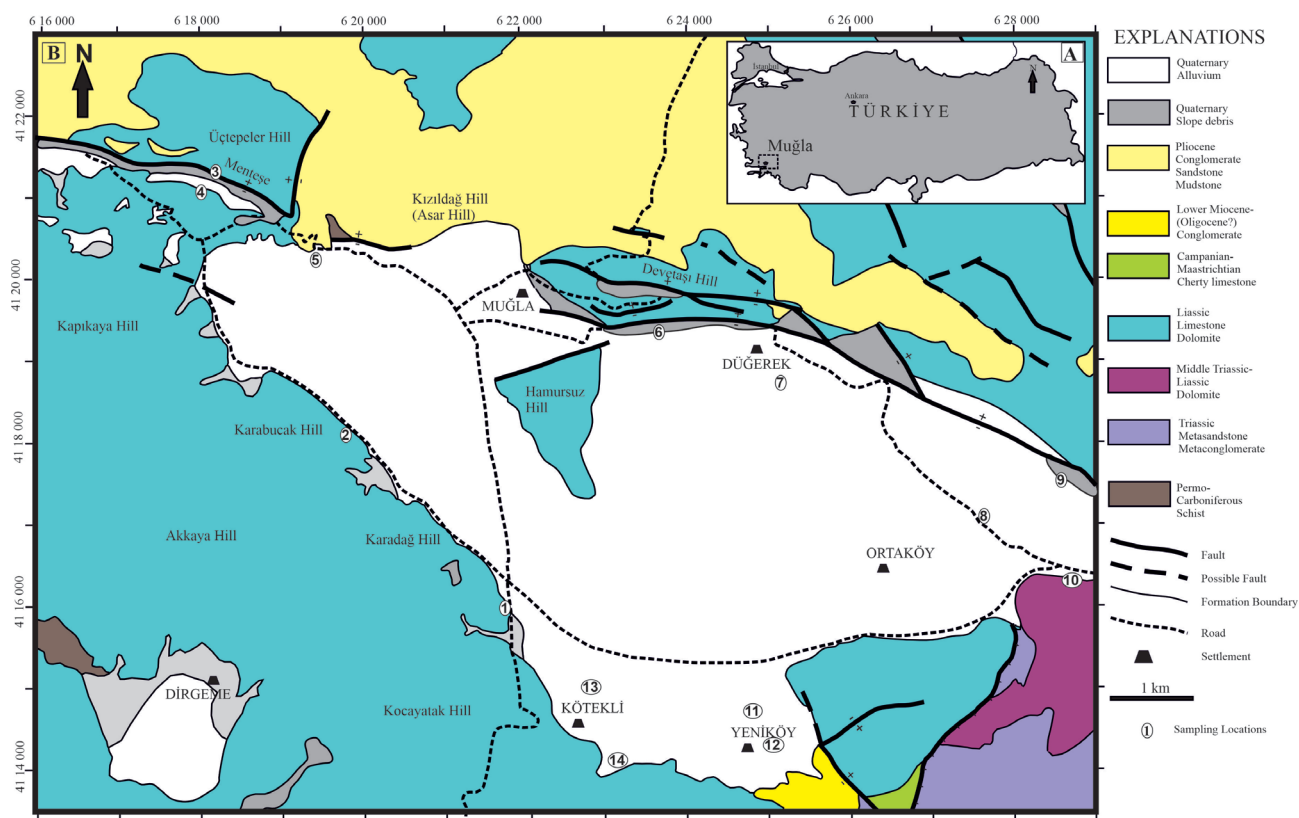


Figure 1. A) Location of the study area in Turkey; B) Geological map of Muğla Polje (Göktaş et al. 1982; Konak et al. 1987; Aktimur et al. 1996; Göktaş 1998).

between 4° and 70° (2θ) and that of oriented samples for the fine fraction ($<2 \mu\text{m}$) were taken between 2° and 42° 2θ upon air-drying, ethylene glycol solvation, and heating to 300 and 550 $^\circ\text{C}$. Mineral identification was based on the combined methods by Thorez (1976); Chen (1977) and Moore and Reynolds (1989); semiquantitative abundances of minerals in bulk compositions were determined using the method by Brindley (1980).

Whole-rock chemical analysis of the parent rocks and the soil samples was performed at Analytical Chemistry Laboratory at MTA by Thermo ARL X-ray fluorescence on powder pellets. The degree of total weathering was quantified using the Chemical Index of Alteration (CIA) equation of Nesbitt and Young (1982) [$\text{CIA} = 100 \times (\text{Al}_2\text{O}_3 / (\text{Al}_2\text{O}_3 + \text{CaO}^* + \text{Na}_2\text{O} + \text{K}_2\text{O}))$] and that of Maynard (1992) [$\text{CIA-K} = 100 \times (\text{Al}_2\text{O}_3 / (\text{Al}_2\text{O}_3 + \text{CaO}^* + \text{Na}_2\text{O}))$]. CaO^* in the silicate fraction was corrected based on the method of McLennan (1993). The climofunction of CIA-K is also used to quantify the mean annual precipitation (MAP) values in mm year^{-1} with an equation of $\text{MAP} = 14.265 (\text{CIA-K}) - 37.632$ (Sheldon et al., 2002). Degree of salinization ($(\text{K}_2\text{O} + \text{Na}_2\text{O}) / \text{Al}_2\text{O}_3$), calcification ($(\text{CaO} + \text{MgO}) / \text{Al}_2\text{O}_3$), clayeyness ($\text{Al}_2\text{O}_3 / \text{SiO}_2$), and base loss (Base / Ti) were calculated and compared with the reference

values according to the given equations in Retallack (2001), Retallack et al. (2002), Sheldon (2006), and Sheldon and Tabor (2009).

3. Results

3.1. Petrography of the parent rocks

The petrographical study was carried out on the parent rocks of the samples. Thin sections prepared from the mid-Triassic-Liassic parent rock (10-D-K) indicate the presence of fine-medium-grained calcite and vein infillings (Figures 3A and 3B). According to Folk (1962) and Dunham (1962) classifications, the parent rock of TRs sample (10-D-K) was defined as dismicrite and crystalline limestone, respectively. Thin sections of the TRs parent rocks (2-, 4-, 14-D-K) show that they contain fine-medium crystalline calcite, rarely fossil remnants and stylolites (Figures 3C and 3D). Thus, they are classified dominantly as dismicrite and to a lesser extent biomicrite in terms of Folk (1962) classification; crystalline limestone and to a lesser extent wackestone according to Dunham (1962). Petrographical investigation on the Oligo-Miocene sandstone (12-D-K) reveals the presence of dominantly fine-medium grained quartz in association with muscovite and opaque minerals (Figures 3E and 3F).

Table 1. Environmental settings of each sampling site in the study area.

Map location	Sample no	Depth (cm)	Coordinates	Parent material	Bedrock	Soil
2	2-D	90	35 61 80 63 E-41 19 454 N	Limestone	Liassic carbonates	Terra rossa
4	4-D	120	35 61 73 31 E-41 20 901 N	Limestone	Liassic carbonates	Terra rossa
10	10-D	70	35 62 84 31 E-41 16 088 N	Dolomitic Limestone	Middle Triassic-Liassic carbonates	Terra rossa
14	14-D	65	35 59 22 74 E-41 33 544 N	Limestone	Liassic carbonates	Terra rossa
1	1-2-D 1-3-D 1-4-D 1-D-PAL	20-40 40-58 58-128 128-	35 61 98 76 E-41 17 500 N	Alluvium	Liassic Carbonates	Alluvium soil
7	7-1-D 7-2-D 7-3-D 7-4-D	0-70 70-110 110-145 145-185	35 62 54 31 E-41 18 707 N	Alluvium	Liassic Carbonates Late Miocene-Pliocene Clastics	Alluvium soil
8	8-1-D 8-2-D 8-3-D 8-4-D	0-40 40-60 60-90 90-130	35 62 71 50 E-41 17 153 N	Alluvium	Liassic Carbonates Late Miocene-Pliocene Clastics	Alluvium soil
11	11-D	60	35 62 46 36 E-41 14 601 N	Alluvium	Lower Miocene-Oligocene Clastics, Liassic Carbonates	Alluvium soil
12	12-1-D 12-2-D	0-50 50-130	35 62 48 30 E-41 13 761 N	Alluvium	Lower Miocene-Oligocene Clastics, Liassic Carbonates	Alluvium soil
13	13-1-D 13-2-D 13-3-D 13-4-D	0-25 25-85 85-140 140-230	35 62 20 13 E-41 15 555 N	Alluvium	Liassic Carbonates	Alluvium soil
6	6-D	340	35 62 45 17 E-41 19 306 N	Colluvium	Liassic Carbonates Late Miocene-Pliocene Clastics	Colluvium-soil
9	9-1-D 9-2-D 9-3-D	0-30 30-100 100-350	35 62 84 42 E-41 17 427 N	Colluvium	Liassic Carbonates Late Miocene-Pliocene Clastics	Colluvium-soil

3.2. Soil properties

The cation exchange capacity of TRs samples ranges between 13 and 16.8 meq/100 g, while ALs and CLs samples have a wider range from 2 to 11.6 and from 7 to 11.6 meq/100g (Table 2). The results show that the dominant clay minerals of all samples have low cation exchange capacities (Grim, 1968). Textural analysis of the soil samples based on USDA (1975) reveals that TRs are classified as clay (with clay greater than 65%) while the texture classes of ALs range between clay to sandy loam (that of ALsc between silty loam and clay) and that of CLs vary from silty clay loam to silty loam (Table 2).

3.3. Mineralogical determinations

Minerals of Pls, TRs, ALs, ALsc, and CLs are identified by using diffraction patterns of bulk samples and clay fractions. Representative diffractograms for each group are given in Figures 4 and 5. Semiquantitative analysis of the bulk compositions and the presence/absence of clay minerals for all samples are listed in Table 3. Quartz is observed in all samples with its prominent peaks at 3.34, 4.26, 2.28, and 1.81 Å as very clear and sharp reflections (Figure 4). It is most abundant (20%–47%) in ALs. Feldspars are the other nonclay components of the samples. Plagioclase is detected by its 3.18–3.21 Å reflections in Pls, ALsc, and

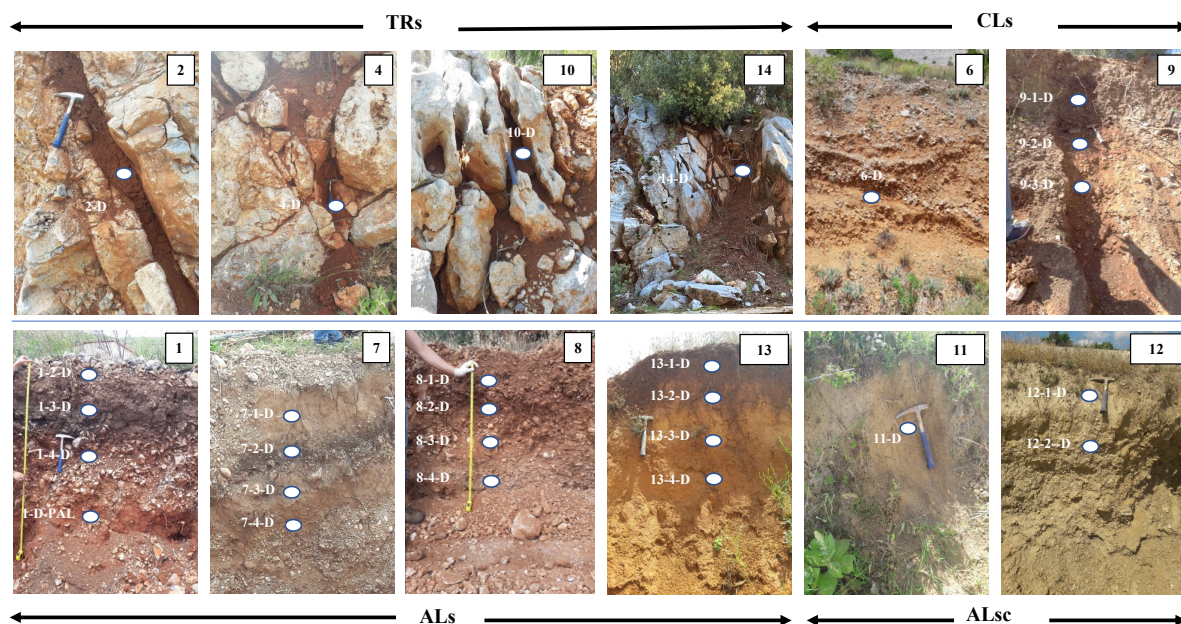


Figure 2. Field photographs of the studied samples and profiles of TRs, CLs, ALs, and ALsc.

CLs (Figure 4). The characteristic peak of K-feldspar at 3.24 Å is only observed in Pls. The total abundance of feldspars is not more than 10% for any sample (Table 3). Calcite appears in the diffractograms of ALs and CLs (32%–97%) as sharp and relatively intense reflections at 3.03 Å while weaker in ALsc (Figure 4). However, it is not determined in Pls and TRs samples. Weak reflection at 2.89 Å is characterized as dolomite for Pls. Hematite is defined in all samples with 2.56 and 2.69 Å peaks with different intensities (Figure 4). Its semiquantity is determined as 5%–7% for TRs; 1%–6% for ALs and CLs (Table 3). Diffractograms of the bulk compositions host wide and weak peaks around 14, 10, and 7 Å associated with the presence of clay minerals. The series of 14, 7, 4.7, and 3.53 Å reflections refer to the presence of chlorite possibly interfering with vermiculite (?). The reflections at 10, 5, and 3.38 Å are characteristic of illite/mica for all samples (Figure 4). The broad 7 Å peak shows more than one mineral sharing the same reflections. $d(060)$ reflections at 1.54 Å refer to the presence of trioctahedral chlorite and vermiculite (?) while 1.49 Å peak points to dioctahedral kaolinite (Figure 4). Total clay content is highest for TRs at 53%–75% followed by Pls with 62%, which reaches 52% max for ALs and 18% max for CLs. Its semiquantity is between 37% and 63% for ALsc. Mica minerals also appear in ALsc samples with an abundance of 7%–12% (Table 3).

Illite is unaffected by ethylene glycol solvation and heating treatments. The characteristic peaks of illite are observed at around 10, 5, and 3.38 Å for Pls, TRs, ALs, ALsc, and CLs (Figures 5A–5E). Basal series of $d(002)$

and (004) for chlorite overlap with (001) and (002) of kaolinite; 002 reflection of kaolinite is observed at around $24.9^\circ 2\theta$ with 3.58 Å while 004 reflection of chlorite shows up at nearly $25.1^\circ 2\theta$ with 3.55 Å. Additionally, 001 and 003 peaks of chlorite are very weak implying its low concentration in all types of samples except ALsc at which both reflections appear more strongly (Figure 5D). Heating chlorite to 550 °C intensifies the 001 reflection and weakens the 002, 003, and 004 peaks (Figures 5B and 5C). At this temperature, kaolinite becomes amorphous and its all reflections disappear (Figures 5A–5E). Since chlorite is mixed with possibly vermiculite, their 001 reflections interfere and create an asymmetrical peak at around 14 Å (Figures 5A–5E). Heating samples to 300 °C causes vermiculite structure to collapse to 10 Å by removing 001 interferences and appears similar to reflections of illite/mica (Figures 5A–5E).

3.4. Geochemical analysis

Major oxide compositions of the samples and the parent rocks (given with a suffix K) are listed in Table 4. The parent rocks of TRs samples are CaO rich (54.3%–55.1%) but SiO₂ (0.4%–0.8%), Al₂O₃ (0.1%–0.4%) and Fe₂O₃ (0.1%) deficient. In contrast, the TRs samples are enriched in SiO₂ (45.9%–55.7%), Al₂O₃ (18.5%–24.3%), and Fe₂O₃ (9%–12.5%).

The representative parent rock of an ALsc sample (12-D-K) has very similar major oxide values to their soils in that SiO₂ content ranges between 73.3% and 77.6%, the compositions of Al₂O₃ and Fe₂O₃ have a very narrow variation in the ranges of 9%–11.8% and 4.6%–5.7 %, respectively. Other ALs which have mostly parent rocks

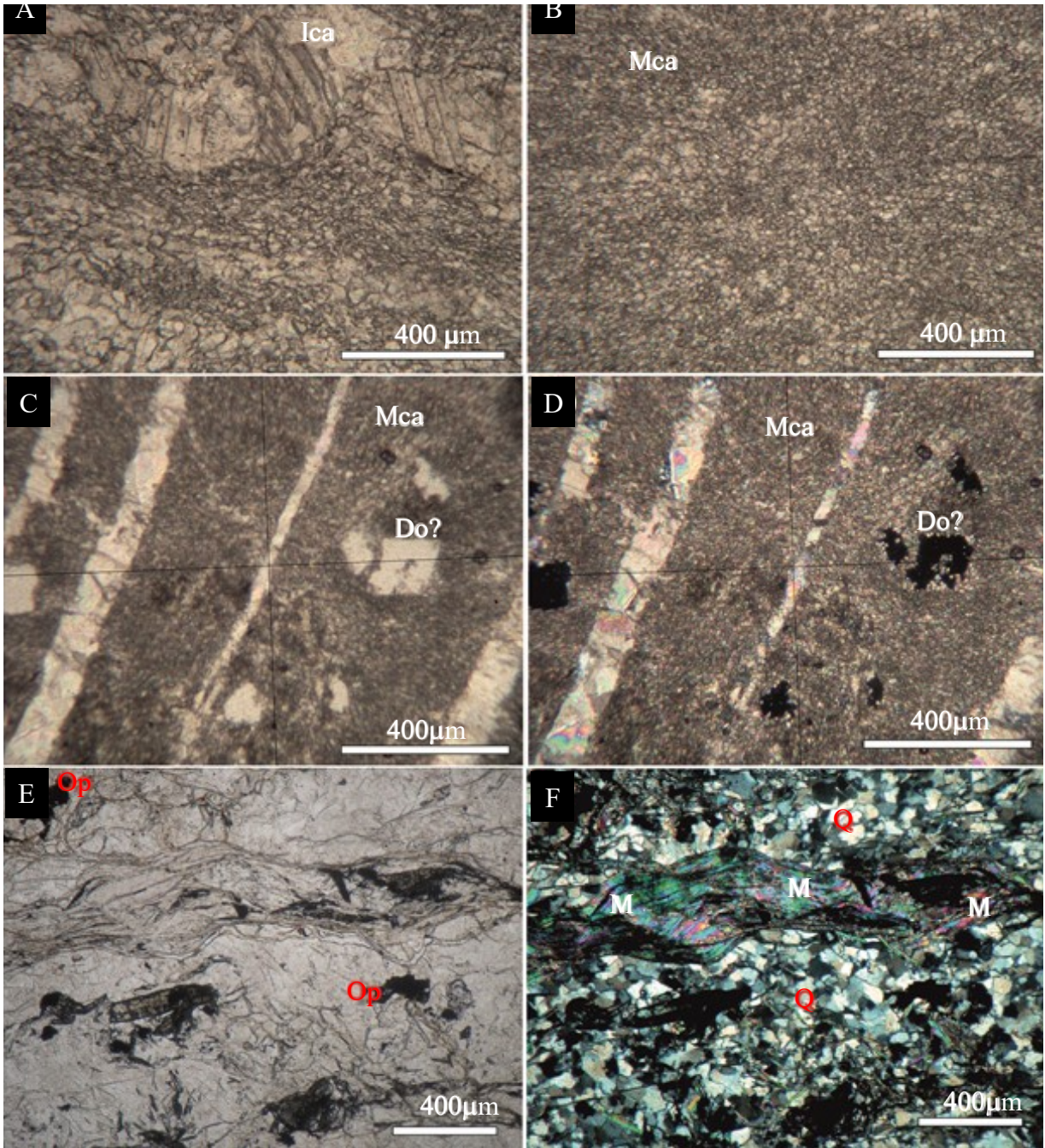


Figure 3. Photomicrographs of the parent rocks A) the Middle Triassic-Liassic limestone showing coarse-crystalline calcite (Ica) filling irregular veins (PPL), B) the Middle Triassic-Liassic limestone with fine-medium- crystalline calcite (Mca) (PPL), C) the Liassic limestone comprising fine-medium- crystalline calcite (Mca) and rhombohedral dolomite (Do) (PPL), D) cross-polarized view of the image c, E) quartz (Q), muscovite (M) and opaque (Op) minerals of the Oligocene?-Lower Miocene clastics (PPL) and f) cross-polarized view of the image.

of carbonate origin have a very low content of SiO_2 and Al_2O_3 (<10%) and Fe_2O_3 (<4.1%) with moderate CaO compositions (33.9%–50.7%).

The same condition exists between CLs and their parent rocks in terms of CaO in that the parent rocks of

CLs (6-, 9-D-K) have CaO content between 54.5% and 54.9%, that of CLs also has a moderate value and a very narrow range (34.9%–41.1%). The composition of SiO_2 is very low (0.5%–1.1%) for the parent rocks (6 and 9-D-K) and could reach up to 17.9% max for CLs. Very low Al_2O_3

Table 2. Sample depth, CEC, particle size distribution of TRs, ALs, ALsc, Pls, and CLs.

Profile no	Sample no	Depth (cm)	Soil	CEC (meq/100g)	Clay (%)	Silt (%)	Sand (%)	Texture class
2	2-D	90	TRs	13.8	67	22.4	10.6	Clay
4	4-D	120	TRs	16.8	85	11.4	3.6	Clay
10	10-D	70	TRs	16.4	81	17.4	1.7	Clay
14	14-D	65	TRs	13	65	23.0	12.0	Clay
1	1-Pal	128	Pls	14.2	72	25	3	Clay
1	1-4	58-128	ALs	6	43.7	47.8	8.5	Silty clay
7	7-1-D	0-70	ALs	9.7	34	35.9	30.6	Clayey loam
7	7-3-D	110-145	ALs	11.6	35	33.6	31.4	Clayey loam
7	7-4-D	145-185	ALs	10.5	35	32.7	32.3	Clayey loam
11	11-D	60	ALsc	2	20	51.3	28.7	Silty loam
12	12-1-D	0-50	ALsc	3	25	57.9	17.1	Silty loam
12	12-2-D	50-130	ALsc	5.2	45	39.1	15.9	Clay
13	13-1-D	0-25	ALs	7.8	47	28	25	Clay
13	13-2-D	25-85	ALs	5.6	32	31	37	Clayey loam
13	13-3-D	85-140	ALs	3	17	27.6	55.4	Sandy loam
13	13-4-D	140-230	ALs	5.6	25	29	46	Loam
6	6-D	340	CLs	11.6	40	40.4	19.6	Silty-clay loam
9	9-2-D	30-100	CLs	7	39	50.4	10.6	Silty-clayey loam
9	9-3-D	100-350	CLs	8.6	17.5	63.3	19.2	Silty loam

and Fe_2O_3 contents are also marked as <8% and <4%, respectively. The weight percentages of MgO (<1.7), NaO (<0.7), K_2O (<1.7), and MnO_2 (<0.5) are very low for TRs, ALs, CLs and their parent rocks.

The molecular weathering ratios based on the major oxide compositions of the soil samples are given in Table 5. CIA and CIA-K values of TRs are greater than 83%. ALsc samples have CIA between 80.5% and 82.5% while their calculated CIA-K values reach up to 93%. The chemical weathering degrees of the rest of the ALs and CLs samples are very low (<22%). The paleosol is very similar to TRs samples with very high degrees of CIA (93%) and CIA-K (93%). The calculated MAP values for TRs, Pls, and ALsc range between 1230 and 1288 mm year⁻¹. However, MAP for ALs is between 6 and 270 mm year⁻¹ while for CLs it is in the range of 111–197 mm year⁻¹. The molecular weathering ratio of salinization is very low (0.1–0.2) for all soil samples. ALs and CLs samples have moderate to high calcification; however, TRs samples are decalcified (0.1–0.2). Clayeyness is not more than 0.7 for all soils samples; however, base loss varies; it appears as a low ratio (3.2–3.8) for TRs, buried soils (3.2) and ALsc (3–4.4). Calculated base loss ratios for ALs and CLs are 72–522, 73–141, respectively.

4. Discussion

Based on the weathering degree, three major classes of soils—TRs, ALs, and CLs—are compared mineralogically and geochemically. The dominant clay mineral for all soils has the property of low CEC. In terms of field occurrences and the particle size, the intensity of leaching decreases in the polje from TRs being the well-drained soil towards ALs and CLs.

Munsell hue shows similar distinctions from TRs (the reddest) with 2.5 YR to ALs and CLs with a range of 2.5–7.5 YR. The soils of this study, TRs, ALs, and CLs include dominantly kaolinite and illite associated with chlorite and vermiculite as the clay minerals of the soils in Muğla Polje. Leaching of Ca^{+2} from top of the profiles towards the lower horizons causes very strong attraction between clay surfaces (Altunbaş and Sarı 2009; Sarı et al., 2018). The exchange between Ca^{+2} released from carbonates and K^+ from the weathering of mica (for ALsc) enhances the transformation of mica to vermiculite (Bassett, 1959). In this respect, the clay mineralogical compositions of TRs, ALs, and CLs are found to be compatible with the compositions of terra rossa developed under Mediterranean climate (Durn et al., 1999; Boero et al., 1992; Macleod, 1980; Garcia-Gonzales and Recio, 1988; Katipoğlu et al., 2015; Altunbaş and Sarı,

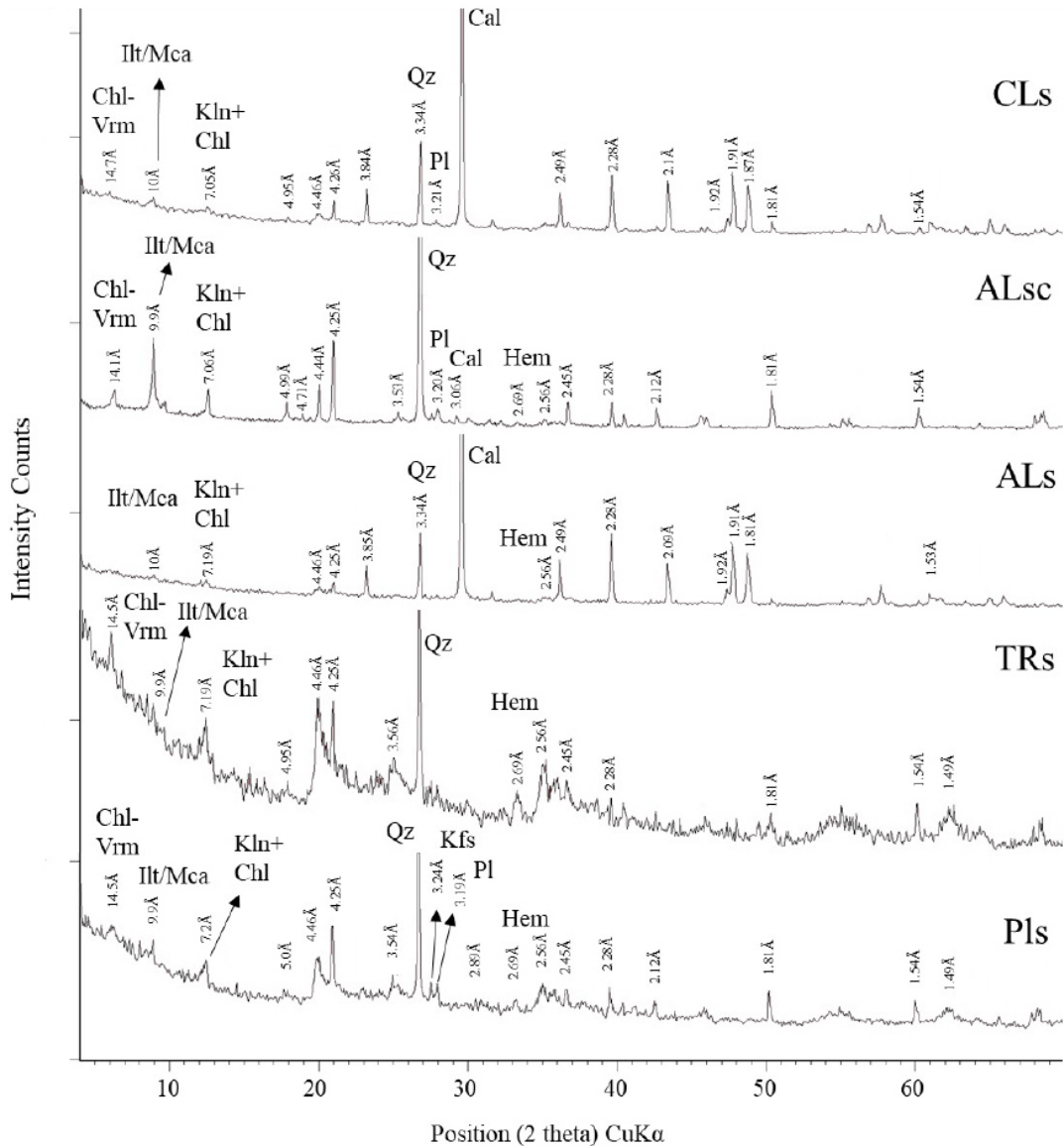


Figure 4. X-ray diffractogram of bulk compositions of Pls, TRs, ALs, ALsc, and CLs (abbreviations of mineral names after Whitney and Evans, 2010).

2009; Cengiz and Kuşcu, 2010). Hematite, the source of red color is found in all soil occurrences within the polje.

Al is selected as the reference phase due to its stability under weathering; therefore, binary plots of selected major oxides were plotted with respect to Al_2O_3 in weight percentages (Figure 6). All binary plots reveal that ALs and CLs plot in very close proximity or along the same line; while TRs and Pls show very similar variations and plot closely. Al_2O_3 in the bulk composition of TRs shows a positive correlation with Fe_2O_3 and K_2O ; a negative correlation with SiO_2 and CaO , and no change with respect to Na_2O and TiO_2 . As weathering intensity increases, only CaO is depleted in the composition of ALs while SiO_2 ,

Fe_2O_3 , K_2O , Na_2O , and TiO_2 show a positive correlation with Al_2O_3 (Figure 6). In terms of Al_2O_3 in CLs; Fe_2O_3 , K_2O , and TiO_2 are positively correlated while CaO and SiO_2 are reversely changed. MgO plots scattering for TRs, ALs, and CLs (Figure 6).

Weathering trends of TRs, ALs, and CLs are also displayed on A-CN-K triangular plot of Nesbitt and Young (1984) (Figure 7). Along the line I, the weathering of ALs samples form a parallel trend to A-CN side of the diagram explaining the initial stage of weathering. Lines II and III show offset from the weathering trend and conversion of kaolinite to illite by K^+ addition. Along line II, CIA does not change remarkably due to the balance between loss

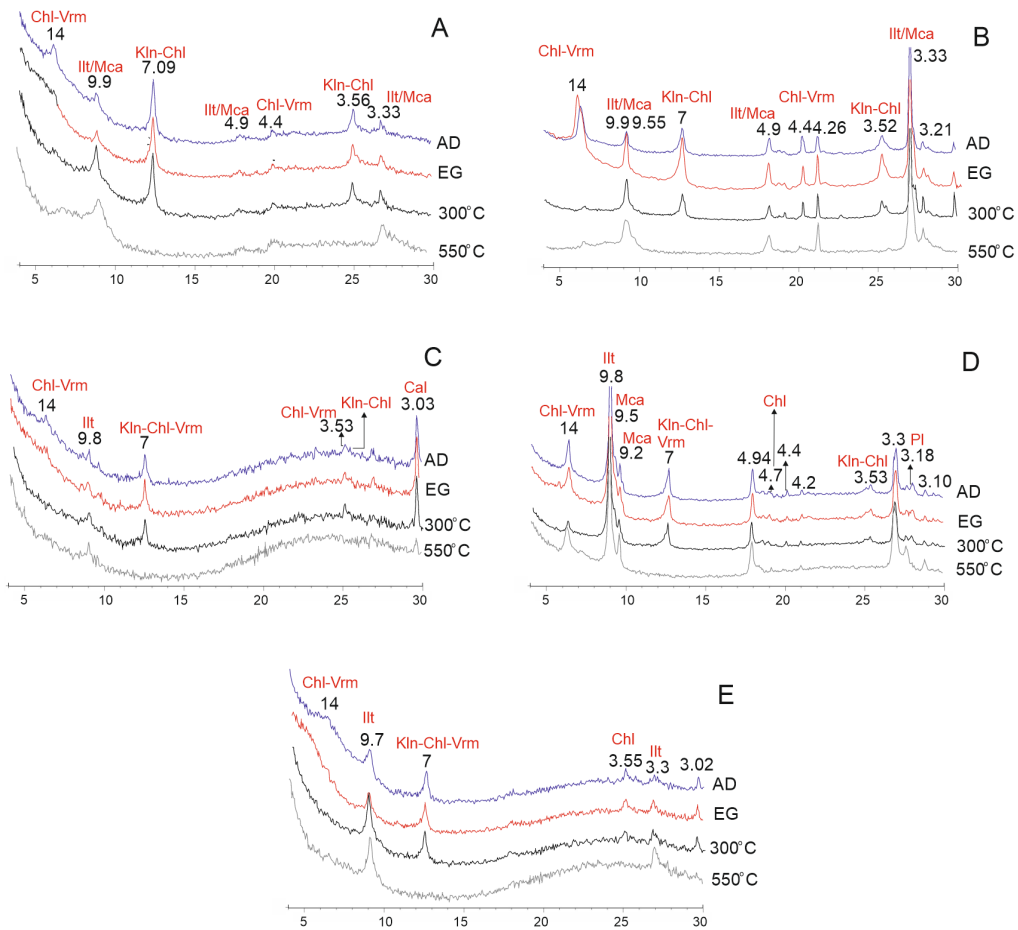


Figure 5. X-ray diffractograms of clay fractions of A) Pls, B) TRs, C) ALs, D) ALsc, and E) CLs (AD: air-dried; EG: ethylene glycol solvated; 300° and 550° C: heated samples; abbreviations of mineral names after Whitney and Evans, 2010).

of alkalis and K^+ addition; it marks the conversion of plagioclase to K-feldspar; while line III marks lower CIA values with greater loss of Ca^{++} and Na^+ but enrichment of K^+ . Line III shows mixing lines representing the conversion of aluminous clay minerals to illite (Fedo et al., 1995). TRs reveal advanced weathering with marked loss in K^+ with the compositional shift towards the Al apex of the diagram (Figure 7).

Molecular weathering ratios of the studied soils are consistent with the soil properties, clay minerals that exist in the composition, and the presence of hematite as a reddening agent for all soils. The low degree of salinization (<1) and calcification (<2), high degree of clayeyness (>0.3), and intense hydrolysis are the characteristics of TRs. All of these molecular weathering ratios are compatible with very high CIA and CIA-K percentages (83.5%–88.4% and 88.9%–92.7%) which hereby point to very high MAP (1230–1285 mm year⁻¹). This, in turn, results in low CEC, low $CaCO_3$, and low alkali-alkaline earth cations, and in situ formation of kaolinite for TRs.

ALsc have very similar properties to TRs in that low degree of salinization (<1) and calcification (<2) with intense leaching (>0.2) associated with very high CIA (>80%) and CIA-K (>90%), all of which favor the clayeyness degree greater than that of ALs developed from carbonate dominant parent rocks. For CLs, moderate to high calcification, very high base amounts, and low degree of leaching are all compatible with low CIA and CIA-K (<17%) and MAP (<200 mm year⁻¹).

The buried soil (Pls/1-D-Pal) that is found in the 1st ALs profile carries much stronger hydrolysis fingerprints than TRs. Low degree of salinization (<1) and calcification (<2), high degree of base loss, and clayeyness (>0.3) are the remarkable molecular weathering ratios for the paleosol.

5. Conclusion

This study classifies the soils of Muğla Polje into three: the first class is terra rossa (TRs) which refers to highly clayey, red-colored soil developed on hard and permeable limestone under very high precipitation leading to

Table 3. Semiquantitative mineralogical analyses of Pls, TRs, ALs, ALsc, and CLs.

Soil	Sample no	Minerals of bulk composition							Minerals of clay fraction		
		Qz	Cal	Fsp	Hem	Mca	Dol	Clay	Kln	Ilt	Chl+Vrm
TRs	2-D	37	1	2	7	-	-	53	+	+	+
TRs	4-D	15	1	3	6	-	-	75	+	+	+
TRs	10-D	27	3	2	5	-	-	63	+	+	+
TRs	14-D	30	1	10	6	-	1	53	+	+	+
ALs	1-2-D-A	7	70	2	2	-	-	19	+	+	+
ALs	1-3-D-B	8	38	1	1	-	-	52	+	+	+
ALs	1-4-D-E	13	68	-	1	-	-	18	+	+	+
ALs	1-D-Pal*	27	-	4	3	-	2	62	+	+	+
ALs	7-1-D	19	56	7	3	-	-	15	+	+	+
ALs	7-2-D	7	70	2	2	-	-	19	+	+	-
ALs	7-3-D	6	71	3	-	-	1	19	+	+	+
ALs	7-4-D	9	75	-	-	-	-	16	+	+	+
ALs	8-1-D	13	65	3	2	-	-	18	+	+	+
ALs	8-2-D	1	87	-	-	-	-	12	+	+	
ALs	8-3-D	3	84	2	-	-	-	11	+	+	+
ALs	8-4-D	3	97	-	-	-	-	-	-	-	-
ALsc	11-D	32	1	4	1	12	1	49	+	+	+
ALsc	12-1-D	47	1	6	-	10	-	37	+	+	+
ALsc	12-2-D	20	5	2	1	8	1	63	+	+	+
ALs	13-1-D	8	32	2	6	7	1	45	+	+	+
ALs	13-2-D	6	69	2	4	-	1	18	+	+	+
ALs	13-3-D	1	84	3	2	-	3	7	+	+	-
ALs	13-4-D	1	83	-	1	-	-	16	+	+	-
CLs	6-D	14	62	3	3	-	-	18	+	+	+
CLs	9-1-D	1	85	-	2	-	-	12	+	+	-
CLs	9-2-D	9	80	1	2	-	-	8	+	+	+
CLs	9-3-D	9	79	-	-	-	1	11	+	-	-

+ refers to the presence of mineral; - refers to either absent or undetected.

high chemical alteration and leaching. TRs can also be named the soils of high lands in the polje. The soils of lowlands are the second and third classes that form the matrix of transported sediments as alluvium-derived soils (ALs) and colluvium-derived soils (CLs). These low

to moderately drained soils are defined by their variable grain sizes, red colors, and moderate calcification ratios developed under low chemical alteration and leaching. Furthermore, two distinct soils developed within the same dynamics of ALs but having more Si-enriched

Table 4. Whole rock major oxide compositions of TRs, ALs, and CLs and some parent materials (*P1-parent rock of TRs/2-, 4-, 10- and 14-D; **P2-parent rock of ALsc/12-D; ***P3-parent rock of CLs/6- and 9-D).

Soil/ bedrock	Sample	SiO ₂	Al ₂ O ₃	TiO ₂	CaO	Fe ₂ O ₃	K ₂ O	MgO	MnO	Na ₂ O	P ₂ O ₅	LOI	Sum
TRs	2-D	51.2	20.8	1.5	2.3	9.0	1.5	1.4	0.2	0.3	0.2	11.2	99.1
P1*	2-D-K	0.5	0.2	<0.1	54.7	0.1	<0.1	0.4	<0.1	0.2	<0.1	43.7	99.9
TRs	4-D	45.9	24.3	1.3	1.6	9.6	1.3	1.1	0.1	0.3	0.2	14.0	99.2
P1*	4-D-K	0.6	0.2	<0.1	54.3	0.1	<0.1	0.6	<0.1	0.2	<0.1	43.8	99.9
TRs	10-D	48.0	21.8	1.2	1.9	12.5	1.3	1.0	0.1	0.3	0.1	11.2	99.0
P1*	10-D-K	0.8	0.4	<0.1	54.7	0.1	<0.1	0.3	<0.1	0.2	<0.1	43.4	100.0
TRs	14-D	55.7	18.5	1.4	1.8	9.4	1.2	1.2	0.5	0.3	0.2	9.7	99.4
P1*	14-D-K	0.4	0.1	<0.1	55.1	0.1	<0.1	0.4	<0.1	0.2	<0.1	43.7	100.0
ALs	1-2-A	14.8	6.2	0.4	38.3	2.6	0.5	1.0	0.1	0.3	0.2	35.3	99.2
ALs	1-3-B	15.8	6.6	0.5	36.9	2.8	0.6	0.8	0.1	0.3	0.2	35.4	99.5
ALs	1-4-E	11.0	4.6	0.3	43.2	1.9	0.4	0.9	<0.1	0.2	0.1	37.3	99.7
Pls	1-D-Pal	50.1	22.4	1.5	1.4	9.6	1.7	1.4	0.2	0.3	0.2	11.1	99.4
ALs	7-1-D	17.8	6.2	0.4	37.9	2.8	0.6	0.6	0.1	0.3	0.1	33.0	99.4
ALs	7-2-D	20.0	7.7	0.5	34.1	3.1	0.7	0.7	0.1	0.3	0.2	32.2	99.1
ALs	7-3-D	15.1	5.5	0.4	40.8	2.5	0.5	0.5	<0.1	0.3	0.1	34.1	99.5
ALs	7-4-D	16.5	6.1	0.4	39.2	2.6	0.6	0.6	<0.1	0.3	0.1	33.5	99.6
ALs	8-1-D	11.6	5.0	0.3	42.9	2.2	0.3	0.5	<0.1	0.3	0.1	36.5	99.4
ALs	8-2-D	5.7	2.3	0.2	49.5	1.0	0.1	0.3	<0.1	0.1	0.1	40.5	99.7
ALs	8-3-D	4.8	1.6	0.1	50.7	0.7	0.1	0.3	<0.1	0.2	0.1	41.4	99.8
ALs	8-4-D	5.5	1.8	0.1	49.8	0.9	0.1	0.4	<0.1	0.2	0.1	41.0	99.7
ALsc	11-D	74.4	11.8	1.1	0.2	5.8	1.6	0.8	0.1	0.7	0.1	3.4	99.2
ALsc	12-1-D	76.5	10.2	0.9	0.4	5.7	1.3	0.8	0.1	0.5	0.1	3.2	99.1
ALsc	12-2-D	77.6	9.9	0.7	0.4	5.4	1.4	0.7	0.1	0.6	0.1	3.0	99.2
P2**	12-D-K	73.3	9.0	1.2	3.5	4.6	1.2	1.7	0.1	0.3	0.1	4.8	99.4
ALs	13-1-D	18.6	9.4	0.5	33.9	4.1	0.8	1.0	0.1	0.3	0.1	30.8	99.2
ALs	13-2-D	10.3	5.3	0.3	43.7	2.2	0.4	0.6	<0.1	0.3	0.1	36.8	99.7
ALs	13-3-D	3.7	1.7	0.1	51.5	0.8	0.1	0.4	<0.1	0.2	<0.1	41.3	99.7
ALs	13-4-D	11.6	4.8	0.3	43.7	2.0	0.4	0.5	<0.1	0.2	0.1	36.3	99.7
CLs	6-D	16.3	4.8	0.3	41.1	2.3	0.4	0.5	0.1	0.2	<0.1	33.9	99.7
P3***	6-D-K	0.5	0.1	<0.1	54.9	0.1	<0.1	0.5	<0.1	0.2	<0.1	43.7	100.0
CLs	9-1-D	11.8	7.9	0.5	40.4	3.3	0.4	0.5	0.1	0.2	0.1	34.7	99.6
CLs	9-2-D	17.9	6.9	0.5	34.9	3.0	0.6	0.7	0.1	0.2	0.2	34.8	99.4
CLs	9-3-D	14.3	7.2	0.4	40.0	2.8	0.4	0.5	0.1	0.2	0.1	34.0	99.7
P3***	9-D-K	1.1	0.2	<0.1	54.5	0.1	<0.1	0.4	<0.1	0.2	<0.1	43.4	100.0

*P1-bedrock of TRs (2-, 4-, 10- and 14-D); **P2-bedrock of ALsc (12-D); ***P3-bedrock of CLs (6- and 9-D).

Table 5. Molecular weathering ratios, chemical index of alteration, and mean annual precipitation values of TRs, ALs, and CLs.

Soil	Sample	CIA (%)	CIA-K (%)	MAP (mm year ⁻¹)	Salinization*	Calcification*	Clayeyness*	Base loss*
TRs	2-D	83.5	88.9	1230	0.1	0.2	0.4	3.7
TRs	4-D	88.4	92.7	1285	0.1	0.1	0.5	3.3
TRs	10-D	86.2	90.8	1258	0.1	0.1	0.5	3.8
TRs	14-D	84.9	89.8	1243	0.1	0.2	0.3	3.2
ALs	1-2-A	13.7	13.8	160	0.1	6.3	0.4	100.3
ALs	1-3-B	14.9	15.1	177	0.1	5.7	0.4	77.2
ALs	1-4-E	9.5	9.6	99	0.1	9.6	0.4	149.0
Pls	1-D-Pal	86.8	92.9	1288	0.1	0.1	0.4	3.2
ALs	7-1-D	13.8	14.0	162	0.1	6.2	0.3	98.5
ALs	7-2-D	18.0	18.3	223	0.1	4.5	0.4	71.6
ALs	7-3-D	11.7	11.8	131	0.1	7.5	0.4	105.3
ALs	7-4-D	13.2	13.4	153	0.1	6.5	0.4	101.8
ALs	8-1-D	10.3	10.4	110	0.1	8.7	0.4	146.7
ALs	8-2-D	4.4	4.4	26	0.1	21.7	0.4	250.0
ALs	8-3-D	3.0	3.0	6	0.2	31.9	0.3	513.0
ALs	8-4-D	3.5	3.5	12	0.2	27.9	0.3	505.0
ALsc	11-D	82.5	92.9	1288	0.2	0.1	0.2	3.0
ALsc	12-1-D	82.3	91.9	1273	0.2	0.1	0.1	3.3
ALsc	12-2-D	80.5	90.8	1258	0.2	0.1	0.1	4.4
ALs	13-1-D	21.2	21.6	270	0.1	3.7	0.5	72.0
ALs	13-2-D	10.7	10.8	116	0.1	8.4	0.5	150.0
ALs	13-3-D	3.2	3.2	8	0.2	30.5	0.5	522.0
ALs	13-4-D	9.8	9.9	103	0.1	9.2	0.4	149.3
CLs	6-D	10.3	10.4	111	0.1	8.7	0.3	140.7
CLs	9-1-D	16.2	16.3	195	0.1	5.2	0.7	83.0
CLs	9-2-D	16.2	16.4	197	0.1	5.2	0.4	72.8
CLs	9-3-D	15.1	15.2	179	0.1	5.6	0.5	102.8

*salinization, calcification, clayeyness, and base loss are unitless.

parent rocks (ALsc) reveal very similar properties to TRs. Mineralogically, the same mineral assemblages with different percentages occur in all weathering suites; geochemically, on the other hand, molecular weathering ratios reveal different weathering intensities progressing

on different parts of the polje. It can be concluded that intense and profound weathering on the carbonate rocks of more stable environments leads to the formation of TRs while the low to moderately intense weathering on dynamic lowlands in Muğla Polje triggers the formation

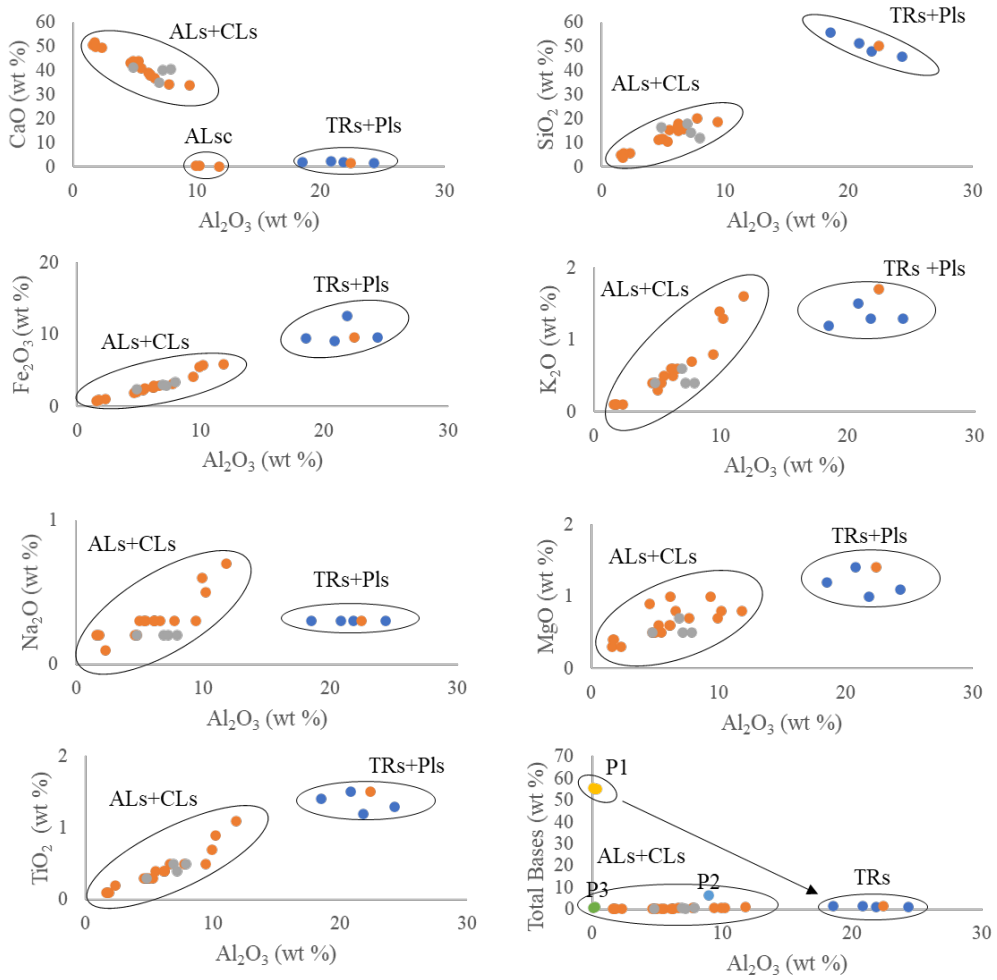


Figure 6. Binary plots of selected major oxides versus Al_2O_3 based on the bulk chemical composition of TRs, ALs (ALsc specifically labeled where it plots separately), CLs samples and Pls

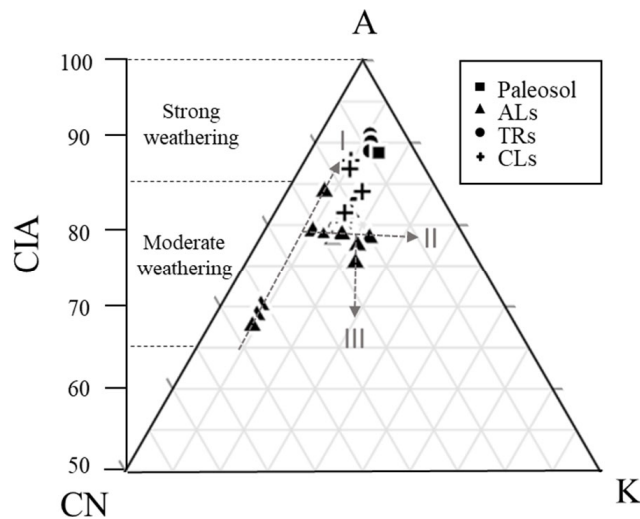


Figure 7. A-CN-K ternary diagram of molecular proportions of $Al_2O_3-(CaO^*+Na_2O)-K_2O$ for TRs, ALs, CLs, and Pls (Nesbitt & Young, 1984) together with the CIA scale along A-CN join. Dashed line I shows the predicted weathering trend; dashed line II refers to the replacement of plagioclase by K-feldspar; dashed line III points to the addition of K^+ to the weathered residues (Fedo et al., 1995).

of ALs and CLs. TRs, being the mature soils of the study area together with the parent rocks, are suggested to be the possible sources of the soils forming the matrix of the transported sediments in lowlands of the polje. Further research on trace element geochemistry of these soils would unlock the relationship between dust contribution and the formation of terra rossa.

References

- Aktimur HT, Özmutaf M, Sariaslan M, Keçer M, Sönmez M et al. (1996). Muğla İlinin (Merkez İlçe) Arazi Kullanım Potansiyeli, MTA Raporu, Rapor No: 9853.
- Altunbaş S, Sarı M (2009). The relationships of iron contents between Red Mediterranean Soils and its parent material in Antalya Province, Turkey. *Akdeniz Üniversitesi Ziraat Fakültesi Dergisi* 22 (1): 15-21.
- ASTM D7928-17 (2017). Standard Test Method for Particle-Size Distribution (Gradation) of Fine-Grained Soils Using the Sedimentation (Hydrometer) Analysis, ASTM International, West Conshohocken, PA.
- Atalay Z (1980). Muğla-Yatağan ve yakın dolay karasal Neojen'inin stratigrafi araştırması. *Türkiye Jeoloji Kurumu Bülteni* 23: 93-99.
- Atalay I (1997). Red Mediterranean soils in some karstic regions of Taurus mountains, Turkey. *Catena* 28 (3-4): 247-260. [https://doi.org/10.1016/S0341-8162\(96\)00041-0](https://doi.org/10.1016/S0341-8162(96)00041-0)
- Aydıncık C, Cresser MS (2008). Red Soils under Mediterranean Type of Climate: their properties use and productivity. *Bulgarian Journal of Agricultural Science* 14 (6): 576-582.
- Aydıncık C, Fitzpatrick E (2009). Pedogenesis and characteristics of the Terra Rossas developed on different physiographic position and their classification. *Agrociencia* 43 (2): 97-105.
- Bassett WA (1959). The origin of vermiculite deposit at Libby, Montana. *American Mineralogist*, 44 (3-4): 282-299.
- Boero V, Schwertmann U (1989). Iron oxide mineralogy of terra rossa and its genetic implications. *Geoderma* 44 (4): 319-327. [https://doi.org/10.1016/0016-7061\(89\)90039-6](https://doi.org/10.1016/0016-7061(89)90039-6)
- Boero V, Premoli A, Melis P, Barberis E, Arduino E (1992). Influence of climate on the iron oxide mineralogy of terra rossa. *Clays and Clay Minerals* 40: 8-13. <https://doi.org/10.1346/CCMN.1992.0400102>
- Bolca M, Altunbaş Ü, Kurucu Y (2012). A study on pedogenetical distribution of minerals in the pedon of rhodoxeralf and rendoll soils showing formation on different slope facets. *Ege Üniversitesi Ziraat Fakültesi Dergisi* 49 (3): 229-238.
- Brindley GW (1980). Quantitative X-Ray mineral analysis of clays G.W. Brindley, G. Brown (Eds.), *Crystal Structures of Clay Minerals and Their X-ray Identification*. Monograph 5, Mineralogical Society, London (1980), pp. 411-438 <https://doi.org/10.1180/mono-5>
- Bronger A, Bruhn-Lobin N (1997). Paleopedology of Terrae rossae-Rhodoxeralfs from Quaternary calcarenites in NW Morocco. *Catena* 28 (3-4): 279-295. [https://doi.org/10.1016/S0341-8162\(96\)00043-4](https://doi.org/10.1016/S0341-8162(96)00043-4)
- Cengiz O, Kuşcu M (2010). Anamasdağları-Isparta terra rossalarının tuğla-kiremit üretiminde kullanılabilirliği. *Kibited* 1 (4): 79-91.
- Chen PY (1977). Table of key lines in X-ray powder diffraction patterns of minerals in clays and associated rocks. *Geological Survey Occasional Paper* 21, Indiana Geological Survey Occasional Paper 21, p 67.
- Whitney DL, Evans BW (2010). Abbreviations for names of rock-forming minerals. *American Mineralogist* 95 (1): 185-187. <https://doi.org/10.2138/am.2010.3371>
- Dunham RJ (1962). Classification of carbonate rocks according to depositional texture. In: Ham, W.E., (eds.): *Classification of carbonate rocks: American Association of Petroleum Geologists Memoir*, pp 108-121. <https://doi.org/10.1306/M1357>
- Durn G (2003). Terra Rossa in the Mediterranean region: parent materials, composition and origin. *Geologia Croatica* 56 (1): 83-100. <https://doi.org/10.4154/GC.2003.06>
- Durn G, Ottner F, Slovenec D (1999). Mineralogical and geochemical indicators of the polygenetic nature of terra rossa in Istria, Croatia. *Geoderma* 91 (1-2): 125-150. [https://doi.org/10.1016/S0016-7061\(98\)00130-X](https://doi.org/10.1016/S0016-7061(98)00130-X)
- Durn G, Čorić R, Tadej N, Barudžija U, Rubinić V et al. (2014). Bulk and clay mineral composition indicate origin of terra rossa soils in Western Herzegovina. *Geologia Croatica* 67 (3): 171-183. <https://doi.org/10.4154/GC.2014.13>
- Eren M, Kadir S (1999). Colour origin of Upper Cretaceous pelagic red sediments within the Eastern Pontides, northeast Turkey. *International Journal of Earth Sciences* 88: 593-595. <https://doi.org/10.1007/s005310050287>
- Eren M, Kadir S (2013). Colour origin of red sandstone beds within the Hüdayi Formation (Early Cambrian), Aydıncık (Mersin), southern Turkey. *Turkish Journal of Earth Sciences* 22: 563-573. <https://doi.org/10.3906/yer-1208-1>
- Fedo CM, Nesbitt HW, Young GM (1995). Unraveling the effects of potassium metasomatism in sedimentary rocks and paleosols, with implications for paleoweathering conditions and provenance. *Geology* 23 (10): 921-924. [https://doi.org/10.1130/0091-7613\(1995\)023<0921:UTEOPM>2.3.CO;2](https://doi.org/10.1130/0091-7613(1995)023<0921:UTEOPM>2.3.CO;2)

- Fedoroff N, Courty MA (2013). Revisiting the genesis of red Mediterranean soils. *Turkish Journal of Earth Sciences* 22 (3): 359-375.
- Feng JL, Pei LL, Zhu X, Ju JT, Gao SP (2018). Absolute accumulation and isotope fractionation of Si and Fe during dolomite weathering and terra rossa formation. *Chemical Geology* 496: 43-56. <https://doi.org/10.1016/j.chemgeo.2018.08.018>
- Folk RL (1962). Spectral subdivision of limestone types. In Ham WE (eds) *Classification of carbonate Rocks-A Symposium*. American Association of Petroleum Geologists Memoir 1: 62-84.
- Garcia-Gonzales MT, Recio P (1988). Geochemistry and mineralogy of the clay fraction from some Spanish Terra Rossa. *Agrochimica* 32 (2-3): 161-170.
- Göktaş F (1982). Muğla yöresindeki Senozoyik yaşlı çökel kayaların sedimentolojik ve paleocoğrafik incelenmesi, MTA Genel Müdürlüğü, Jeoloji Etütleri Dairesi Arşiv No: 519.
- Göktaş F (1998). Muğla çevresindeki (GB Anadolu) Neojen tortullaşmasının stratigrafisi, sedimantolojisi ve bölgesel korelasyonu. MTA Derleme Rapor No: 10225.
- Göktaş F, Alkanoğlu E, Yücelal A, Yalçın L (1982). 1/100 000 ölçekli sayısal jeoloji haritası Aydın N20 paftası. Türkiye Jeoloji Veri Tabanı, Jeoloji Etütleri Dairesi Başkanlığı, MTA Genel Müdürlüğü, Ankara.
- Grim RE (1968). *Clay Mineralogy*. McGraw-Hill, New York.
- Gül M (2015). Lithological properties and environmental importance of the Quaternary colluviums (Muğla, SW Turkey). *Environmental Earth Sciences* 74: 4089-4108. <https://doi.org/10.1007/s12665-015-4506-4>
- Gül M, Karacan E, Aksoy ME (2013). Muğla Kenti Yerleşim Alanı ve Yakın Çevresinin Genel Jeolojik ve Mühendislik Jeolojisi Özelliklerinin Araştırılması (An investigation of general geologic and engineering geological properties of Muğla and surroundings). Muğla Sıtkı Kocman University, Research Fund Project, BAP 12-54, p 28.
- Gül M, Çetin E, Küçükuyşal C, Gülcan M, Kahveci Y (2021). Recent alluvial fan developments in Muğla (SW Turkey). *Arabian Journal of Geosciences* 14: 819. <https://doi.org/10.1007/s12517-021-07159-3>
- Jones FO (1964). New fast accurate test measures bentonite in drilling mud. *Oil and Gas Journal* 42: 76-78.
- Kapur S, Ağlagül S, Karaman C, Şenol M, Atalay I et al. (1993). Dating of red Mediterranean soils in relation to weathering. In Kapur S, Derici MR, Mermut AR, Gülüt KY, Erenolu EB, Akça E, Onaç I (ed), 2nd International Meeting on "Red Mediterranean Soils", Adana. Short Papers and Abstracts. Çukurova University Faculty of Agriculture Publication 44, Adana.
- Katipoğlu D, Hakbilen S, Kavas S, Öner S, Çaputçu A et al. (2015). Değnek ve Tırtar (Mersin) köylerinin çevresinde yeralan Terra-Rossa Topraklarının Kil Mineralojisi ve Jeokimyası - İlk Bulgular. 16. Ulusal Kil Sempozyumu, Çanakkale, pp 166-198.
- Konak N, Akdeniz N, Öztürk EM (1987). Geology of the South of Menderes Massif: IGCP Project No.5: Correlation of Variscan and Pre-Variscan Events of the Alpine-Mediterranean Mountain Belt. Field Meeting, Turkey, Guide Book For the Field Excursion Along Western Anatolia, Turkey, 42-53, Ankara.
- Kubilay N, Saydam AC, Yemencioğlu S, Ağlagül S, Karaman C et al. (1993). Atmospheric dust in southern Turkey. In Kapur S, Mermut AR, Derici MR (ed) 2nd International Meeting on "Red Mediterranean Soils", Adana, pp 45-47.
- Macleod DA (1980). The origin of the red Mediterranean soils in Epirus, Greece. *Journal of Soil Science* 31 (1): 125-136. <https://doi.org/10.1111/j.1365-2389.1980.tb02070.x>
- Lucke B (2008). Demise of the Decapolis. Past and Present Desertification in the Context of Soil Development, Land Use, and Climate. Saarbrücken, Germany, VDM.
- Maynard JB (1992). Chemistry of modern soils as a guide to interpreting Precambrian paleosols. *Journal of Geology* 100 (3): 279-289. <https://doi.org/10.1086/629632>
- McLennan SM (1993). Weathering and Global Denudation. *Journal of Geology* 101: 295-303. <https://doi.org/10.1086/648222>
- Merino E, Banerjee A, Dworkin S (2006). Dust, terra rossa, replacement and karst: serendipitous geodynamics in the critical zone. *Geochimica Cosmochimica Acta* 70: A416. <https://doi.org/10.1016/j.gca.2006.06.837>
- Miko S, Durn G, Prohić E (1999). Evaluation of terra rossa geochemical baselines from Croatian karst regions. *Journal of Geochemical Exploration* 66 (1-2): 173-182. [https://doi.org/10.1016/S0375-6742\(99\)00010-2](https://doi.org/10.1016/S0375-6742(99)00010-2)
- Moore DM, Reynolds RC (1989). *X-ray Diffraction and the Identification and Analysis of Clay Minerals*. Oxford University Press, Oxford.
- Moresi M, Mongelli G (1988). The relation between the terra rossa and the carbonate free residue of the underlying limestones and dolostones in Apulia, Italy. *Clay Minerals* 23 (4): 439-446. <https://doi.org/10.1180/claymin.1988.023.4.10>
- Muhs DR, Budhan JR, Prospero JM, Skipp G, Herwitz SR (2012). Soil genesis on the island of Bermuda in the Quaternary: The Importance of African Dust Transport and Deposition. *Journal of Geophysical Research* 117: F03025. <https://doi.org/10.1029/2012JF002366>
- Nesbitt HW, Young GM (1982). Early Proterozoic climates and plate motions inferred from major element chemistry of lutites. *Nature* 299: 715-717. <https://doi.org/10.1038/299715a0>
- Nesbitt HW, Young GM (1984). Prediction of Some Weathering Trends of Plutonic and Volcanic Rocks Based on Thermodynamic and Kinetic Considerations. *Geochimica et Cosmochimica Acta*, 48 (7): 1523-1534. [https://doi.org/10.1016/0016-7037\(84\)90408-3](https://doi.org/10.1016/0016-7037(84)90408-3)
- Özbek H, Kapur S, Dinç U (1976). Mineralogical Variations Between Two Miocene Dolomitic Limestones and The Overlying Weathered Materials Forming Terra Rossas In Adana Southern Turkey. Çukurova University Ziraat Faculty Publications 7 (2): 118-144.

- Priori S, Costantini EAC, Capezzuoli E, Protano G, Hilgers A, Sauer D, Sandrelli F (2008). Pedostratigraphy of Terra Rossa and Quaternary geological evolution of a lacustrine limestone plateau in central Italy. *Journal of Plant Nutrition and Soil Science* 171 (4): 509-523. <https://doi.org/10.1002/jpln.200700012>
- Retallack GJ (2001). *Soils of the Past: An Introduction to Paleopedology*. Second Edition, Blackwell. <https://doi.org/10.1002/9780470698716>
- Retallack GJ, Wynn JG, Benefit BR, Mccrossin ML (2002). Paleosols and paleoenvironments of the middle Miocene, Maboko Formation, Kenya. *Journal of Human Evolution* 42 (6): 659-703. <https://doi.org/10.1006/jhev.2002.0553>
- Sandler A, Meunier A, Velde B (2015). Mineralogical and chemical variability of mountain red/brown Mediterranean soils. *Geoderma* 239-240: 156-167. <https://doi.org/10.1016/j.geoderma.2014.10.008>
- Sarı M, Kurucu Y, Akça E, Eren M, Kadir S et al. (2018). Luvisols. In: Kapur S., Akça E., Günel H. (eds) *The Soils of Turkey*. World Soils Book Series. Springer, Cham. https://doi.org/10.1007/978-3-319-64392-2_15
- Schoeneberger PJ, Wysocki DA, Benham EC, Soil Survey Staff (2012). *Field book for describing and sampling soils*, Version 3.0. Natural Resources Conservation Service, National Soil Survey Center, Lincoln, NE.
- Sheldon ND, Retallack GJ, Tanaka S (2002). Geochemical climofunctions from North America soils and application to paleosols across the Eocene-Oligocene boundary in Oregon. *Journal of Geology* 110: 687-696 <https://doi.org/10.1086/342865>
- Sheldon ND (2006). Abrupt chemical weathering increase across the Permian-Triassic boundary. *Palaeogeography, Palaeoclimatology, Palaeoecology* 231 (3-4): 315-321. <https://doi.org/10.1016/j.palaeo.2005.09.001>
- Sheldon ND, Tabor NJ (2009). Quantitative paleoenvironmental and paleoclimatic reconstruction using paleosols. *Earth-Science Reviews* 95 (1-2): 1-52. <https://doi.org/10.1016/j.earscirev.2009.03.004>
- Soil Survey Staff (1975). *Soil Taxonomy: A Basic System of Soil Classification for Making and Interpreting Soil Surveys*. USDA Handbook No. 436. US Government Printing Office, Washington, DC.
- Soil Survey Staff (1992). *Keys to soil taxonomy*, sixth edition (1994).
- Thorez J (1976). *Practical Identification of Clay Minerals*. Lelotte, Disson, Belgium.
- Torrent J (2005). Mediterranean soils. In Hillel D (ed), *Encyclopaedia of Soils in the Environment*. vol. 2. Elsevier Academic Press, Oxford, pp 418-427. <https://doi.org/10.1016/B0-12-348530-4/00023-0>
- Vingiani S, Di Iorio E, Colombo C, Terribile F (2018). Integrated study of Red Mediterranean soils from Southern Italy. *Catena* 168: 129-140. <https://doi.org/10.1016/j.catena.2018.01.002>
- Wei X, Ji H, Li D, Zhang F, Wang S (2013). Material source analysis and element geochemical research about two types of representative bauxite deposits and terra rossa in western Guangxi, southern China. *Journal of Geochemical Exploration* 133: 68-87. <https://doi.org/10.1016/j.gexplo.2013.07.010>
- IUSS Working Group WRB (2015). *World Reference Base for Soil Resources 2014, update 2015 International soil classification system for naming soils and creating legends for soil maps*. World Soil Resources Reports No. 106. FAO, Rome.
- Yaalon DH (1997). Soils in the Mediterranean region: what makes them different? *Catena* 28 (3-4): 157-169. [https://doi.org/10.1016/S0341-8162\(96\)00035-5](https://doi.org/10.1016/S0341-8162(96)00035-5)
- Yassoglou N, Kosmas C, Moustakas N (1997). The red soils, their origin, properties, use and management in Greece. *Catena* 28 (3-4): 261-278. [https://doi.org/10.1016/S0341-8162\(96\)00042-2](https://doi.org/10.1016/S0341-8162(96)00042-2)